

# Frequency Selection in Heaving Airfoil Wakes Using a High-Order Method

W. Medjroubi<sup>\*1</sup>, J. Peinke<sup>2</sup>

ForWind Center of Wind Energy Research, Institute of Physics, University of Oldenburg  
Ammerländer Heerstr. 136, 26129 Oldenburg, Germany

<sup>\*1</sup>w.medjroubi@uni-oldenburg.de

## Abstract

In this contribution, the unsteady, viscous and two dimensional flow over a plunging NACA0012 airfoil was simulated using a high-order numerical method associated with a moving frame of reference technique. The goal of using a high-order numerical method is to characterize heaving airfoil wakes with very fine temporal and spatial resolutions. This characterization is essential in understanding the transition process experienced by oscillating airfoils and which can enable more control on the transition. The response of motionless and periodically forced airfoils was considered separately. The flow was investigated at a mean incidence  $\alpha = 0^\circ$ , Reynolds number  $Re = 10^4$ , and over a range of heaving frequencies and amplitudes. The resulting airfoil wakes were analyzed with respect to their frequency response and type. It is shown that for forced airfoils three regimes of frequency response exist: a natural regime, a lock-in regime, and a harmonic regime. The transition between these regimes was presented at constant frequency and constant amplitude of the forcing oscillations. The frequency regimes were then explored in detail and related to the wake types and to the wakes transition. The results obtained were in accordance with previously published experimental and computational investigations. Furthermore, a more detailed wake classification was presented, where two more wake configurations were captured. The role of the trailing- and leading-edges in the creation of multiple-vortices-per-half-cycle shedding mode was investigated. Moreover, the interaction of the natural shedding frequency of the airfoil with the imposed forcing frequency and their contribution in the creation of multiple-vortices-per-half-cycle shedding mode was also investigated. These results showed that frequency interactions can be related to the appearance of the multiple-vortices-per-half-cycle modes.

## Keywords

*Computational Fluid Dynamics; Boundary Layer; Oscillating Airfoils; Spectral/Hp Element Methods; Moving Frame Of Reference; Thrust Generation; Frequency Selection; Strouhal Frequency*

## Introduction

Oscillating airfoils have received much attention and

interest in different contexts and applications due to the unsteadiness and the complex nature of these flows, rendering their numerical simulation very challenging. Unsteadiness and its consequences are fundamentally important problems which concern a broad range of applications. These undesirable consequences can range from flutter (Scalan 1971), to vortex-induced-vibrations (VIV) (Williamson 2004), and flow-induced-vibrations (FIV) (Belvin 1977; Naudascher 1994).

Oscillating airfoils include: heaving (or plunging), pitching and flapping airfoils. Purely heaving airfoils have received less attention compared to pitching airfoils, which is mainly due to the applications involving dynamic stall on helicopters which are more concerned by the pitching motion. Nevertheless, heaving airfoils exhibit a rich variety of wakes which are classified into three types as drag-producing, neutral and thrust-producing wakes (Freytmuth 1988; Lai 1999; Young 2005; Medjroubi 2011b; Medjroubi 2012), depending on the frequency and amplitude of the heaving oscillations. At low reduced frequencies, the wake is a Karman vortex street, and the wake produces drag; while at high reduced frequencies, the wake becomes a reversed Karman vortex street. During the transition from drag to thrust-producing wakes, a neutral mode appears where the produced thrust equals the inherent drag. In some cases, this mode is characterized by the shedding of more than one vortex pair per oscillation cycle. This shedding is referred to as the multiple-vortex-per-half-cycle mode. The details of the wake structure formation, and the lift and drag production are not well understood, especially the multiple-vortex-per-half-cycle mode (Young 2001; Young 2005). The multiple-vortex-per-half-cycle mode origin is thought to be the result of the interaction between the natural shedding of the airfoil and the imposed heaving frequency (Young 2005; Medjroubi 2012).

The forced wake of the airfoil exhibits also three

different frequency regimes. These regimes depend on the forcing frequency (and the forcing amplitude) and the relation between the forcing frequency and the natural shedding frequency of the airfoil. The natural frequency (or Strouhal frequency) is defined as the frequency of shedding of vortices of the unforced airfoil (Young 2005; Karniadakis 1989). The three regimes exhibited are called natural, harmonic, and lock-in regimes, and have been extensively studied and observed for oscillating cylinders (Ongoren 1988a; Ongoren 1988b; Karniadakis 1989; Cheng 2001; Young 2004), but less explored for oscillating airfoils (Young 2005; Young 2004). The objective of this paper is to explore these regimes and to determine the relation between the frequency regimes and the wake types.

Spectral/hp Element Methods was used in this work combined with a moving-frame of reference technique to investigate the problem of the flow around an oscillating airfoil (Medjroubi 2011b). All the simulations presented in this work are Direct Numerical Simulations (DNS), in order to capture all the flow details and particularly the spatio-temporal flow evolution. To the authors knowledge, it is the first time that the frequency-regimes were investigated for a heaving airfoil using a high-order numerical approach, as most of the studies for this type of motion were concerned with the wake configuration (Young 2005; Anderson 1998; Ellenrieder 2003).

In this paper, the incompressible, 2D and unsteady flow over a stationary and a heaving NACA0012 airfoil was simulated. The Reynolds numbers considered are moderate ( $Re=10^4 - 3 \times 10^4$ ), with Re number based on the airfoil chord length). A range of heaving amplitudes and frequencies was simulated in order to expose the frequency regimes introduced earlier and to achieve a transition between these regimes. The dependency of the frequency regimes on the relation between the natural and forcing frequency was explored as the origin of the multiple-vortex-per-half-cycle shedding mode. The Spectral /hp Element Method and the moving-frame of reference technique are introduced in Section 2. The characterization of the wake modes in function of the interaction of the natural shedding frequency and the imposed heaving frequency interaction are presented in Section 3. Finally, Section 4 contains a summary of the findings of this paper.

### The Numerical Method

The main idea behind using high-order numerical methods is to achieve high accuracy, resolving all the

flow length scales at a reduced cost and avoiding the extra costs of remeshing or excessive grid resolution (Nastase 2006). Unlike pure spectral methods and finite elements methods, Spectral/hp Element Methods (SEM) allows the use of two refinement techniques simultaneously: the h-refinement, denoting the increase of the number of elements, and the p-refinement, denoting the increase of the polynomial order of the approximation (Karniadakis 2005). The p-refinement is a powerful tool, as it offers the possibility of increasing the simulations accuracy without any remeshing by increasing the order of the approximation in all or parts of the computational domain, which can be considered as a way of implementing adaptivity. For more details about the derivation and applications of SEM, the reader can refer to (Karniadakis 2005; Karniadakis 1991; Medjroubi 2011a). To implement the airfoil motion, the Navier-Stokes equations and the boundary conditions were written in a moving frame of reference. In the following, the principles of the Spectral/hp Element Method and the moving frame of reference are presented. Readers interested in the details of the derivation and the implementation of the method can refer to the monograph by S. Sherwin and G. Em. Karniadakis (Karniadakis 2005).

### Spatial and Spectral Discretization

The 2D Navier-Stokes equations for an incompressible, unsteady and viscous flow are written as:

$$\nabla \cdot \mathbf{u} = 0, \tag{1}$$

$$\frac{\partial \mathbf{u}}{\partial t} + (\mathbf{u} \cdot \nabla) \mathbf{u} = -\frac{\nabla p}{\rho} + \nu \nabla^2 \mathbf{u} + \mathbf{F}, \tag{2}$$

where:  $\mathbf{u}$  is the velocity vector,  $p$  the pressure,  $\nu$  the kinematic viscosity and  $\mathbf{F}$  are the body forces.

The physical domain is divided into triangular and/or quadrilateral (tetrahedral and/or hexahedrals) sub-domains for 2D (3D) configurations. A spectral expansion in the form of Jacobi polynomials of mixed weight and of order  $p$ , was used to represent the solution variable within each sub-domain.

### Polynomial Bases/Expansions

For a polynomial expansion, a basis  $u_{m,n}(r,s)$  needs to be defined in order to approximate the function  $f(x,y)$  over  $i$  triangular sub-domains using a  $C^0$  continuous expansion of the form (for basis used for rectangular sub-domains refer to (Karniadakis 2005)):

$$f(x,y) = \sum_i^N \sum_m^{N_1} \sum_n^{N_2} u_{m,n}^i(r(x,y),s(x,y)) \tag{3}$$

where:  $u_{m,n}^i$  are the expansion coefficients in the  $i^{th}$  sub-domain,  $(x, y)$  are the spatial coordinates and  $(r, s)$  are the local coordinates within the sub-domains.  $N$  is the total number of sub-domains,  $N_1, N_2$  are the number of the quadrature points used in the  $r$  and  $s$  directions; respectively. The space spanned by the local coordinates system is defined as follows:

$$L^2 = \{(r, s) \mid -1 \leq r, s; r + s \leq 0\} \quad (4)$$

where the orthogonal expansion bases used are Dubiner's modified bases, defined as:

$$u_{m,n} = P_m^{0,0} \left( 2 \frac{(1+r)}{1-s} - 1 \right) (1-s)^m P_n^{2m+1,0}(s). \quad (5)$$

$P_n^{\alpha,\beta}(x)$  is the  $n^{th}$ -order Jacobi polynomial in the  $[-1,1]$  interval, which satisfies the orthogonality relationship:

$$\int_{-1}^1 P_m^{\alpha,\beta}(x) P_n^{\alpha,\beta}(x) (1-x)^\alpha (1+x)^\beta dx = \delta_n^m, \quad (6)$$

where:  $\delta_n^m$  is the Kronecker-delta.

The bases are decomposed into boundary and interior modes, thus allowing the construction of a global  $C^0$  expansion. Integration and differentiation were performed at element level, and an element-mapping which allows the generalization of the local operations in a standard region to elements of general shapes is defined. To extend these techniques to a  $C^0$  multi-dimensional basis, global operations as matrix numbering, connectivity and assembly were introduced. This spatial discretization thereby introduced is independent from the Navier-Stokes solver. The solver used in this work will be introduced in the next section.

### Navier-Stokes Solver: High Order Splitting Scheme

The temporal discretization of the Navier-Stokes equations was achieved via a splitting scheme. This temporal scheme requires three steps to determine the fields for the next time step using the velocity at the previous time step. The linear terms in the Navier-Stokes equation are treated implicitly, while the nonlinear terms are treated explicitly. A Poisson equation is solved for the pressure, and this is achieved by forcing the incompressibility constraint over an intermediate velocity field. The final velocity field is obtained by solving a Helmholtz equation. For more details about this scheme, refer to (Karniadakis 1991).

### The Dimensionless Navier-Stokes Equations

The non-dimensional Navier-Stokes equations were

obtained by making use of the following dimensionless variables:

$$x^* = \frac{x}{c}, \quad y^* = \frac{y}{c} \quad (7)$$

$$t^* = \frac{tU_0}{c}, \quad u^* = \frac{u}{U_0} \quad (8)$$

$$v^* = \frac{v}{U_0}, \quad p^* = \frac{p}{\rho U_0^2}, \quad (9)$$

where:  $U_0$  is the free-stream velocity,  $c$  is the chord length of the airfoil,  $u$  and  $v$  the horizontal and vertical velocity components. The Reynolds number is defined as  $Re = \frac{U_0 c}{\nu}$ .

After introducing the non-dimensional variables, the dimensionless Navier-Stokes equations are obtained:

$$\nabla \cdot \mathbf{u}^* = 0, \quad (10)$$

$$\frac{\partial \mathbf{u}^*}{\partial t} + (\mathbf{u}^* \cdot \nabla) \mathbf{u}^* = -\nabla p^* + \frac{1}{Re} \nabla^2 \mathbf{u}^*. \quad (11)$$

For simplification the  $*$  sign is dropped.

### Airfoil Motion

To implement the oscillatory motion of the airfoil, the Navier-Stokes equations are written in a moving frame of reference and an equation is derived for the airfoil motion. The resulting system is then solved. The method is shortly described here, and for further details, refer to (Li 2002).

Consider that the airfoil performs a translational motion  $d(t)$  defined in the fixed or absolute frame of reference  $(X_a, Y_a)$ :

$$d = (a(x), b(y)). \quad (12)$$

A moving frame of reference is then attached to the airfoil,  $(x_m, y_m)$  which can be defined as a function of the absolute frame as:

$$X_a = a(x) + x_m, \quad (13)$$

$$Y_a = b(x) + y_m. \quad (14)$$

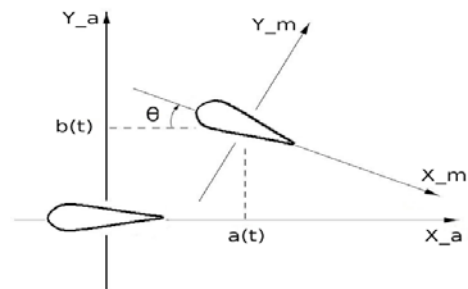


FIG. 1 SCHEMATIC REPRESENTATION OF THE AIRFOIL FOR THE HEAVE MOTION, WHERE THE VERTICAL DISPLACEMENT  $y(t)$  VARIES SINUSOIDALLY.  $\theta$  IS THE MEAN INCIDENCE (INITIAL ANGLE OF ATTACK),  $U_\infty$  IS THE FREE-STREAM VELOCITY AND  $c$  THE CHORD LENGTH.

Using the definition of the coordinates  $(x_m, y_m)$  given by the equations (13) and (14), the Navier-Stokes equations are then re-written in the moving frame of reference as:

$$\nabla \cdot \mathbf{u} = 0, \quad (15)$$

$$\frac{\partial \mathbf{u}}{\partial t} + (\mathbf{u} \cdot \nabla) \mathbf{u} = -\nabla p + \frac{1}{\text{Re}} \nabla^2 \mathbf{u} + Q(u, t), \quad (16)$$

$$Q(u, t) = -A^T \ddot{d}, \quad (17)$$

where:  $A^T \ddot{d}$  results from the unsteady translational motion. The boundary conditions are also written in the moving frame of reference, and expressions are derived for Neumann and Dirichlet boundary conditions. For the present simulations, the airfoil is considered as rigid and forced to oscillate in heave motion as illustrated in Figure 1. The heave motion is defined as:

$$d(t) = y(t) = y_0 + a \cos(2\pi ft). \quad (18)$$

where:  $y(t)$  is the time dependent vertical motion,  $y_0$  is the initial heaving amplitude,  $f = f^* = fc / U_\infty$  and  $a$  the dimensionless frequency and amplitude of oscillations; respectively.

The airfoil is set at a constant initial angle of attack  $\alpha$  and forced to oscillate vertically in a sinusoidal fashion. The boundary conditions at the domain surfaces are inflow conditions at the entry of the domain and outflow conditions at the domain exit. Periodic boundary conditions were used for the upper and lower part of the domain. The boundary conditions at the airfoil surface are no-slip conditions.

### Flow Solver

The general purpose Navier-Stokes solver Nektar was used, based on the Spectral /hp Element Method. The solver was validated for many flow geometries, among those cylindrical (Carmo 2008) and rectangular (Li 2002). The solver was validated for the airfoil geometry for steady and unsteady flows (Medjroubi 2001b; Medjroubi 2011a; Medjroubi 2012) and the results obtained were in agreement with previously published numerical results (Shatalov 2006; Lian 2007; Gopalan 2008) was found. All the simulations of oscillating airfoils were started from fully converged motionless airfoil solutions.

### Results

The results presented here were obtained using a 2D unstructured grid composed of 4220 elements. Details

about the numerical grid, the boundary conditions used and the parameters of the SEM method can be found in (Medjroubi 2011b).

### Unforced Airfoil Wakes

The flow is simulated at  $\alpha = 0^\circ$  and at a Reynolds numbers  $\text{Re} = 10^4$ . The flow exhibits a typical Karman vortex-street configuration, attached over all the surface of the airfoil and leaves the airfoil parallel to the trailing-edge. The vortices are shed at a certain distance from the trailing-edge due to the wake instability (Schnipper 2009) and this distance decreases as the Reynolds number is increased. The wake is a drag-producing wake, and this is confirmed by the value of the mean thrust coefficient.

A Fast Fourier Transform (FFT) was performed on the time series  $u(t)$  at  $\text{Re} = 10^4$  and  $\alpha = 0^\circ$  in order to obtain its frequency content. This technique was used to characterize the frequency content of the airfoil response either for the motionless airfoil or for the heaving airfoil. Fig. 2 illustrates the FFT of the time trace of the horizontal velocity  $u(t)$ . The peak frequency  $k = k_{nat} = 7.85$  is called the natural shedding frequency, or frequency at which the vortices are shed into the wake of the airfoil. It characterizes the response of the airfoil to the incoming inflow at a certain Reynolds number (Green 1995). The frequency response contains also some other weaker peaks at the superharmonics of the natural shedding frequency. This behavior is typical of a motionless object response to an incoming inflow (Blevins 1977; Karniadakis 1989; Williamson 1995; Mittal 1999).

### Forced Airfoil Wakes

The response of the airfoil wake to a harmonic forcing was presented in this Section. The airfoil was forced to oscillate in heave at a prescribed frequency and amplitude at  $\text{Re} = 10^4$  and a mean angle of attack  $\alpha = 0^\circ$ . The imposed heaving frequency was labeled forcing frequency,  $k_f$ . The response frequency of the flow to forcing was obtained by analyzing the frequency content of the temporal signal of the horizontal velocity  $u(t)$  using a FFT. The dominant frequency in the response signal was labeled  $k_r$ . The frequency and amplitude values considered in this simulation were chosen to exhibit the heaving airfoil wake in different frequency-response regimes.

These regimes are the natural regime, where the response frequency is equal to the natural shedding

frequency of the motionless airfoil. The lock-in regime corresponds to the response frequency locked to the forcing frequency. Finally, the harmonic regime corresponds to the response frequency being a mixture of the natural and the forcing frequency.

**Constant Frequency Regime Transition**

The forcing frequency was kept constant and the forcing amplitude was varied. The frequency content of the horizontal velocity time signal was extracted at a location in the near wake ( $x= 1.63, y= 0.09$ ) and its frequency content was then determined by performing an FFT. This location was chosen according to the assumption that it is in the near wake that the forcing and natural frequency compete with each other. The result of this frequency competition or interaction determined the final state of the wake (Karniadakis 1989).

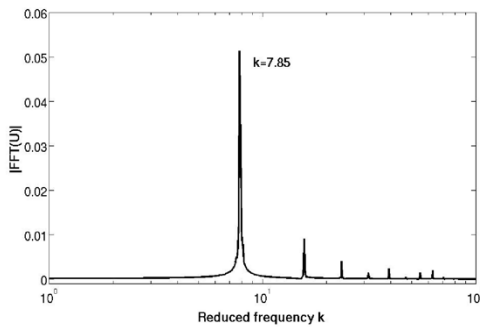
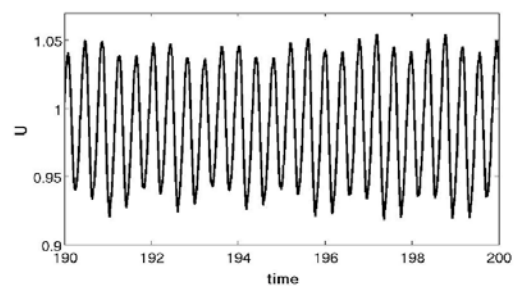


FIG. 2 FAST FOURIER TRANSFORM OF  $u(t)$  FOR A MOTIONLESS AIRFOIL AT  $Re = 10^4$  AND  $\alpha = 0^\circ$ .

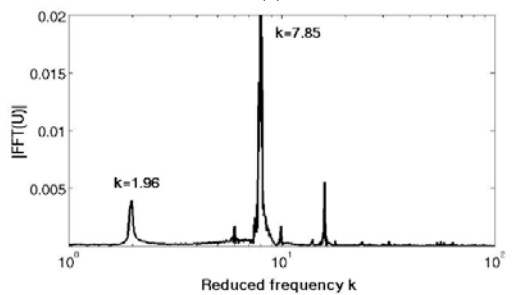
The time trace of the horizontal velocity and the FFT analysis of the natural regime (or mode) are shown in Fig. 3a and Fig. 3b. This regime was obtained at  $k = 1.96$  (corresponding to  $k / k_{nat} = 1/4$ ) and  $h = 0.001$ . The dominant peak occurred at a frequency equal to the natural shedding frequency  $k_{nat} = 7.85$  and its first super-harmonic. Another peak occurred at the forcing frequency but weaker than the ones at  $k_{nat}$  and its super-harmonic. Some other weak peaks were present around the dominant peaks, and this behavior was also observed for a cylinder in a non-lock-in state and reported in (Karniadakis 1989). Increasing the forcing amplitude to  $h = 0.04$  and keeping the frequency of oscillation constant have resulted in a dramatic change in the frequency response of the flow. Fig. 3c shows the time-series of  $u$  and Fig. 3d shows its FFT analysis. The peak frequency is  $k_r = 5.93$  corresponding to a linear combination of the natural shedding frequency and the forcing frequency ( $k_r = k_{nat} / 2 + k_f$ ), which

indicates a harmonic regime where  $k_{nat}$  and  $k_f$  interact together. The result of this interaction is that the peak frequency is some mixture of the natural shedding frequency and the imposed forcing frequency. Other weaker peaks are present at some other combinations of these two frequencies ( $k_{nat} + k_f, 1/4 k_{nat} + k_f$ ).

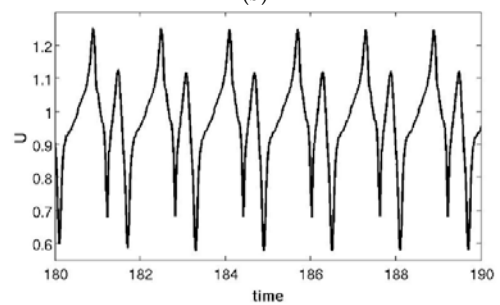
Compared to the frequency response of the natural regime, it is important to note that the  $k_r$  peak becomes more important and the peak corresponding to the natural shedding frequency  $k_{nat}$  is less prominent, indicating that the forcing frequency gains importance at the expense of the natural shedding frequency.



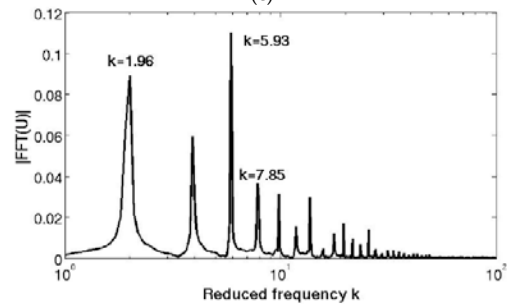
(a)



(b)



(c)



(d)

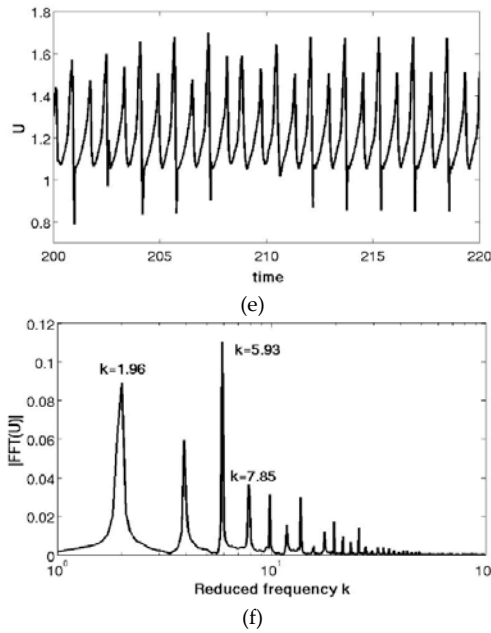


FIG. 3(A) TIME TRACE OF THE HORIZONTAL VELOCITY  $u$  AND ITS (B) FAST FOURIER TRANSFORM  $h = 0.001, k = 1.96$ . (C) TIME TRACE OF  $u$  AND ITS (D) FAST FOURIER TRANSFORM AT  $h = 0.04, k = 1.96$ . (E) TIME TRACE OF  $u$  AND ITS (F) FAST FOURIER TRANSFORM AT  $h = 0.1, k = 1.96$ . ALL SIMULATIONS ARE AT  $Re = 10^4, \alpha = 0^\circ$ , AND  $u(t)$  IS PLOTTED AT THE LOCATION ( $x = 1.63, y = 0.09$ ).

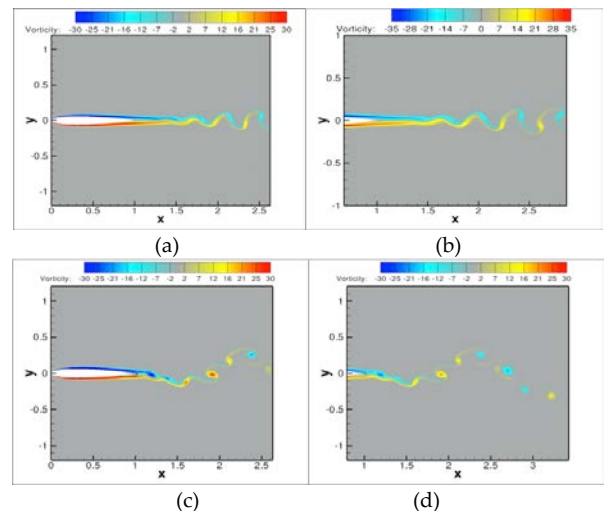
A further increase in the forcing amplitude to  $h = 0.1$  results in a lock-in regime where the response frequency is locked to the forcing frequency. Fig. 3e illustrates the time trace of the horizontal velocity  $u$ . Fig. 3f shows the FFT of the time trace of  $u$  where the peak frequency now corresponds to the forcing frequency  $k_f = k_r = 1.96$ . There are less important peaks at the super-harmonics of the forcing frequency. This is typical for a lock-in regime, as this regime is similar to the non-forced case in its frequency response (see Fig. 2) (Karniadakis 1989).

The frequency regime transition described above embodies another transition in the wake type (or pattern). This transition is from a drag-producing wake to a thrust-producing wake via a neutral wake at constant frequency. Fig. 4 shows the vorticity distributions of the simulations described above. These wake types are typical of heaving airfoils and the transition between them has been reported in the literature (Lai 1999; Young 2004; Young 2005; Platzer 2008; Medjroubi 2011b; Medjroubi 2012). In Fig. 4a, the wake exhibits a Karman vortex-street, where a pair of counter-rotating vortices is shed per oscillation cycle. This is a drag-producing wake. The wake type changes as the amplitude of the heaving oscillation increases (see Fig. 4c). This wake type is called a neutral wake, as the inherent drag balances the

produced thrust.

This wake is also labeled multiple-vortices-per-half-cycle mode, as more than one vortex-pair is shed per oscillation cycle. This mode is not well understood, and the mechanism by which more than a vortex is shed per half-cycle is not well known (Young 2005).

It was proposed here that this mode (or wake type) results from the interaction between the shedding frequency and the imposed frequency, as already explained earlier in this Section by means of FFT analysis. This result will be further confirmed by the simulations of the frequency transition at constant amplitude in the next Section. This explanation for the multiple-vortices-per-half-cycle regime was also provided by Young (Young 2005) who briefly discussed this mode and did not provide any frequency analysis, and then concluded only based on observation of the time trace of  $u$  for one cycle of oscillations. A further increase of the forcing amplitude results in a transition to a thrust-producing wake (see Fig. 4e). Note here that more than one pair of counter-rotating vortices is shed per oscillation-cycle. This thrust-producing wake is different from the typical thrust-producing wake, as the latter looks like the drag-producing wake in Fig. 4a. This new thrust-producing wake is due to the increase in the amplitude of the heaving oscillation. The increase in the amplitude triggers the shedding of more vortices per oscillation cycle (Young 2004). This is mainly due to the fact that at higher amplitudes the leading-edge also contributes to the vortices shed at the trailing-edge. This is confirmed by the presence of vortices on the upper and lower airfoil surface. Note that for the multiple-vortices-per-half-cycle for the neutral regime (see Fig. 4c) there are no contributions from the leading-edge, although the flow is slightly detached close to the trailing-edge region.



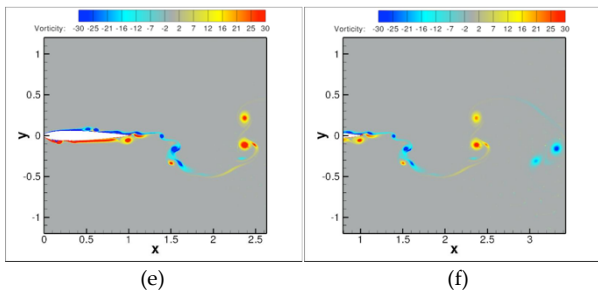


FIG. 4 VORTICITY DISTRIBUTION AT  $A = 0^\circ$ ,  $RE = 104$  FOR (A) A DRAG-PRODUCING WAKE ( $k = 1.96$ ,  $h = 0.001$ ), (B) VIEW OF THE NEAR WAKE REGION. (C) A NEUTRAL WAKE ( $k = 1.96$ ,  $h = 0.04$ ), (D) VIEW OF THE NEAR WAKE REGION. (E) A THRUST-PRODUCING WAKE ( $k = 1.96$ ,  $h = 0.1$ ), (F) VIEW OF THE NEAR WAKE REGION.

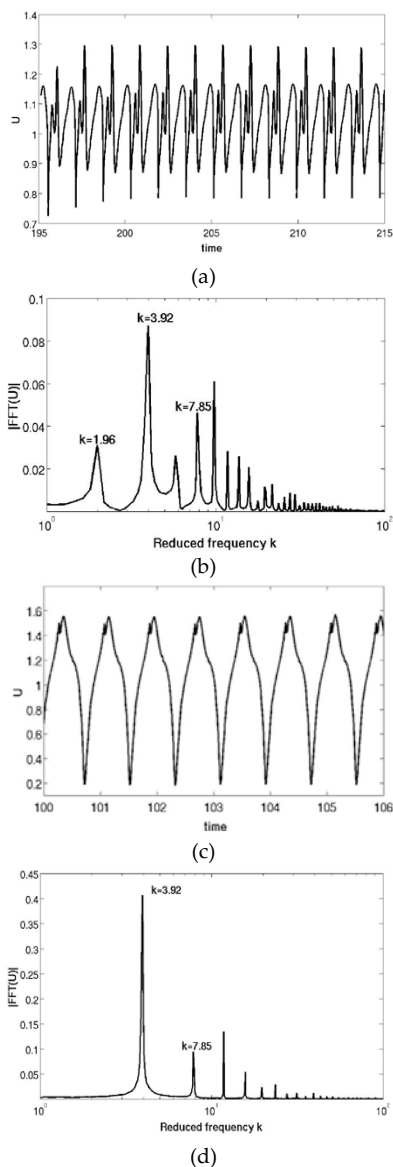


FIG. 5 (a) TIME TRACE OF THE HORIZONTAL VELOCITY  $u$  AND ITS (b) FAST FOURIER TRANSFORM AT  $k = 1.96$ ,  $h = 0.05$ . (c) TIME TRACE OF THE HORIZONTAL VELOCITY  $u$  AND ITS (d) FAST FOURIER TRANSFORM AT  $k = 3.92$ ,  $h = 0.05$ . ALL SIMULATIONS ARE AT  $RE = 10^4$ ,  $\alpha = 0^\circ$ , AND  $u(t)$  IS PLOTTED AT THE LOCATION ( $x = 1.63$ ,  $y = 0.09$ ).

### Constant Amplitude Regime Transition

In this Section, the forcing amplitude is kept constant at  $h = 0.05$  and the forcing frequency is increased. The frequency content of  $u(t)$  is analyzed at the same location as for the constant frequency regime transition.

The time trace of  $u$  at  $h = 0.05$  and  $k = 1.96$  is illustrated in Fig. 5a. The peak frequency of the time trace of  $u$  corresponds to a mixture of the natural shedding frequency and the forcing frequency ( $k_r = 1/4 k_{nat} + k_f = 3.92$ ). A second frequency peak corresponds to another combination of these frequencies ( $k_r = 1/2 k_{nat} + k_f = 5.88$ ) (see Fig. 5b).

There are weaker peaks at the natural shedding frequency and the forcing frequency and their sum ( $k = k_{nat} + k_f = 9.81$ ). This response is typical of a harmonic regime, as shown earlier in this paper for the simulation at ( $k = 1.96$ ,  $h = 0.04$ ). However, it is important to note that for the present simulation ( $k = 1.96$ ,  $h = 0.05$ ) the peak at the natural frequency  $k_{nat} = 7.85$  is more important than the one at the forcing frequency  $k_f = 1.96$ , while this is inverted for the simulation at ( $k = 1.96$ ,  $h = 0.05$ ). This may indicate that the response of the airfoil to the forcing motion depends on the amplitude of the oscillations.

Increasing the forcing frequency to  $k_f = 3.92$  results in a transition to a lock-in regime (see Fig. 5d), where the dominant frequency peak is equal to the forcing frequency  $k_r = 3.92$ . The time trace of the velocity is presented in Fig. 5c. During the transition from the harmonic to the lock-in regime, a wake transition occurs from a neutral to a thrust producing wake. The vorticity contours of the neutral wake (not presented here) show that the wake presents a multiple-vortices-per-half-cycle regime. As for the constant frequency transition, the neutral multiple-vortices-per-half-cycle regime has no vortices contribution from the leading-edge. The flow is attached over all the airfoil surface. The apparition of this mode in the harmonic region, in both simulations at constant forcing frequency and constant forcing amplitude, confirms that the origin of this mode is related to the natural and forcing frequencies interaction. Increasing the frequency of oscillations results in a wake transition to a thrust-producing wake (not presented here). In the wake, one pair of counter-rotating vortices is shed per oscillation cycle. The wake configuration is typical of a thrust-producing wake (Young 2001; Young 2005), and

although there is a slight contribution of leading-edge to the shed vortices, this does not result in a multiple-vortices-per-half-cycle configuration. This phenomenon is discussed in the next Section.

**Frequency Regimes Classification – a Frequency Pattern?**

Several simulations were conducted at different combinations of frequency and amplitude of the forcing oscillations in order to obtain a frequency regime classification. The simulations were conducted at low heaving amplitudes and at moderate to high heaving frequencies. This region of the  $k/k_{nat}$  vs  $h$  plot is associated with aero-elastic and aeroacoustic phenomena and has been not well explored in the literature. The classification was obtained by identifying the different frequency regimes using the FFT analysis and expressed in function of the amplitude and the oscillation frequency normalized by the natural frequency of vortex shedding,  $k/k_{nat}$  (see Fig. 6).

At low forcing frequencies ( $h < 10^{-2}$ ), an increase in the frequency at a constant amplitude triggers a transition from the natural regime to the lock-in regime without going through a harmonic regime. This is also valid for a transition varying the amplitude at a constant forcing frequency for  $k/k_{nat} > 0.5$ . This is because above  $k/k_{nat} = 0.5$ , any harmonic of the forcing frequency will be higher than the natural shedding frequency and the flow will lock to the forcing frequency. This is mainly due to the trailing-edge of the airfoil which dictates the separation point for  $k/k_{nat} > 0.5$  and enforces the dominance of the forcing frequency (lock-in) even in the presence of leading-edge vortex shedding, as it is observed in the case of the constant amplitude regime transition described in Section 3.2.2. The vorticity contours at  $h = 0.05$  and  $k = 3.92$  (corresponding to  $k/k_{nat} = 0.5$ , represented on Fig. 6 with a star pointed to by a red arrow), not presented here, show that vortices are shed at the trailing-edge when the airfoil is at its maximum  $y_{max}$  and minimum  $y_{min}$  vertical position. This is an indication that the trailing-edge motion imposes the shedding process, even if vortices are present at both the upper and lower airfoil surfaces.

Fig. 7 shows the vorticity contours of the wake at  $h = 0.1$  and  $k = 1.96$  ( $k/k_{nat} = 0.25$ , represented by a black circle pointed to by a red arrow on Fig. 6). The shedding of vortices occurs not only when the airfoil is

at  $y_{max}$  or  $y_{min}$  but also when the airfoil is at  $y = 0$ . This explains how more than one vortex-pair is shed per oscillation cycle. In this regime the trailing-edge heaving motion does not control the shedding process. It was believed that the interaction between the natural shedding frequency and the imposed frequency is responsible for this particular shedding regime. The response frequency in this regime that is  $k = 1.24$ , can be written as a combination of both  $k_{nat}$  and  $k_f$ . On the other hand, and when the streamlines were plotted around the trailing-edge region (see Fig. 8), a recirculation region was observed on both sides of the trailing-edge during the whole heaving cycle. This circulation region varies in strength and position during the heaving cycle, thus creating a blunt-like body configuration at the trailing-edge. The variation of this bluntness with the heaving cycle has a frequency associated with it. This frequency be neither the natural nor the forcing frequency but a mixture of both.

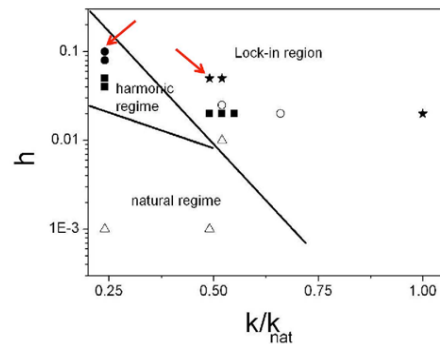
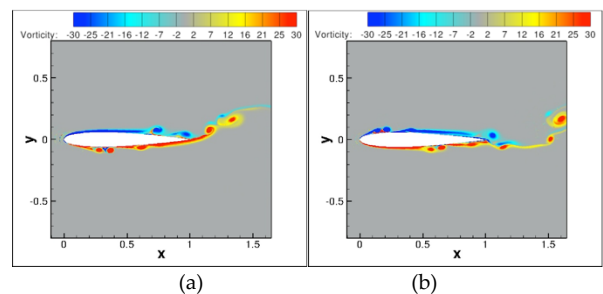


FIG. 6 CLASSIFICATION OF THE WAKE-TYPES AS A FUNCTION OF THE AMPLITUDE  $h$  AND THE NORMALIZED FORCING FREQUENCY  $k/k_{nat}$ . THE TRIANGLES ARE FOR DRAG-PRODUCING WAKES, WITH ONE VORTEX PAIR SHED PER OSCILLATION CYCLE. THE STARS REPRESENT THRUST-PRODUCING WAKES WITH ONE VORTEX PAIR SHED PER OSCILLATION CYCLE. THE SQUARES ARE FOR NEUTRAL WAKES WITH MULTIPLE-VORTICES-PER-CYCLE SHEDDING. THE OPEN CIRCLES REPRESENT NEUTRAL WAKES WITH ONE VORTEX PAIR SHED PER OSCILLATION CYCLE. FINALLY, THE BLACK CIRCLES ARE FOR THRUST-PRODUCING WAKES WITH MULTIPLE-VORTICES-PER-CYCLE SHEDDING. THE FREQUENCY REGIMES BOUNDARIES ARE APPROXIMATELY INDICATED BASED ON THE SIMULATIONS PERFORMED IN THIS PAPER.





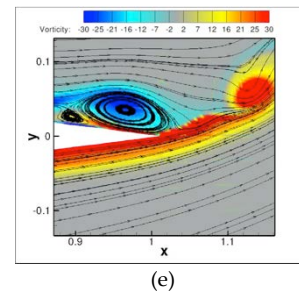
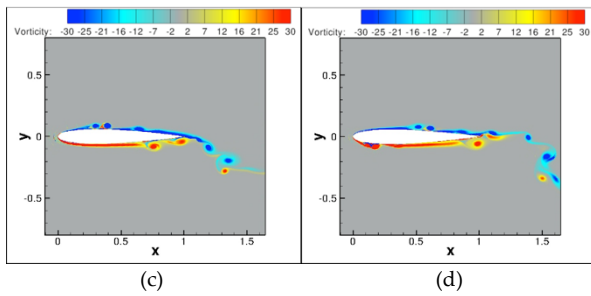


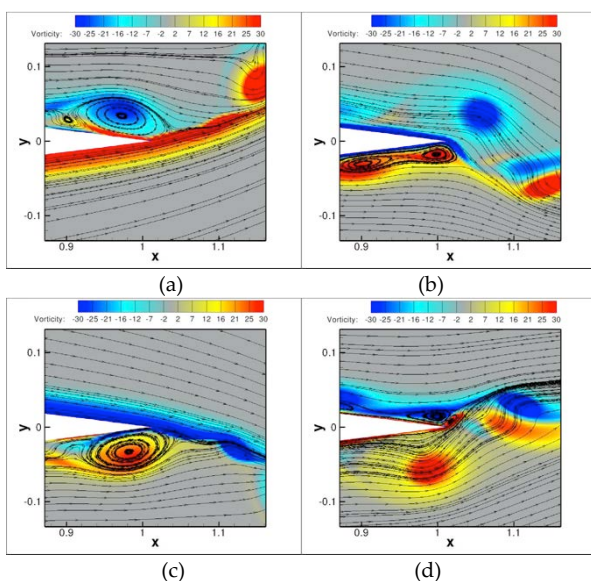
FIG. 7 VORTICITY CONTOURS AT  $\alpha = 0^\circ$ ,  $Re = 10^4$ . THE HEAVING AMPLITUDE IS  $h = 0.1$  AND THE FREQUENCY IS  $k = 1.96$ . THE FIGURES FROM (A) TO (D) REPRESENT ONE HEAVING CYCLE, AND  $Y$  IS THE VERTICAL POSITION OF THE TRAILING-EDGE. (A)  $Y=0$ , (B)  $Y = y_{min}$ , (C)  $Y=0$ , (D)  $Y = y_{max}$ .

FIG. 8 STREAMLINES AT  $\alpha = 0^\circ$ ,  $Re = 10^4$ ,  $h = 0.1$  AND  $k = 1.96$  DURING ONE OSCILLATION CYCLE. (A)  $Y=0$ , (B)  $Y = y_{min}$ , (C)  $Y=0$ , (D)  $Y = y_{max}$ , (E)  $Y=0$ .

In the region defined by  $h > 10^{-2}$  and  $k / k_{nat} < 0.5$ , the transition at constant frequency or amplitude from the natural to the lock-in regime passes via the harmonic regime, as observed in the previous Section.

The classification of the different wakes in terms of the frequency regimes provides an idea of the complexity of the frequency regimes transition and the frequencies interplay in the case of a heaving airfoil. There is a rich variety of wake-types and frequency regimes. It can be concluded that the wake-type is strongly related to the frequency regime. For example, wake-types with multiple-vortices-per-half-cycle of oscillation are in a region where the force and the natural frequency of vortex shedding interact together (the harmonic regime). Wake-types with one vortex-pair shed per cycle are in the region where one distinct frequency is in control.

Note also that the phase diagram is not symmetric, as it is the case for the cylinder (Karniadakis 1989; Young 2005). This can be attributed to the presence of the sharp trailing-edge of the airfoil.



The wake classification presented in this paper agrees very well with the one presented by J. Young in (Young 2005) at  $Re = 2 \times 10^4$ , although the author noted the presence of only three wake types in his diagram and no frequency analysis was presented to confirm the nature of the frequency regimes. A less similar diagram for the pitching airfoil was shown by T. Schnipper et al. (see (Schnipper 2009), Fig.2). Although it is important to note that for both the pitching and heaving cases, there exist a region where the shedding of more than a vortex pair per oscillation occurs and that this region is confined to high amplitudes and low oscillation frequencies.

### Conclusion

The simulations of two dimensional unsteady flow on both a motionless and a heaving airfoil using a high-order spectral CFD method were successful. The high spatial and temporal resolution achieved by the Spectral /hp Element Method permitted a detailed analysis of the flow over the airfoil and the near wake. The high-order numerical methods enabled the simulation and the characterization of the frequency response regimes. These regimes are: (a) the natural regime, (b) the lock-in regime, and (c) the harmonic regime. These frequency-response regimes are related to the shedding process through which the wake undergoes a transition from a Karman street (a drag-producing wake) to a reversed Karman street (a thrust-producing wake). The transition between the different frequency regimes was simulated at both constant frequency and constant amplitude. This transition is successfully related to the wake-types regimes and the transition between them. It has been found that the frequency regimes are strongly related to the wake type exhibited. Wake-types with multiple-vortices-per-half-cycle of oscillation were found in harmonic regimes and wake-types with one vortex-pair shed per cycle were in the region where one distinct frequency was in control (lock-in and natural

regimes). Regimes where the leading-edge vortices contribute to the shedding process were also simulated.

#### ACKNOWLEDGMENT

The authors gratefully acknowledge the computer time provided by the Regionales Rechenzentrum für Niedersachsen (RRZN). W.M. was supported by a DAAD scholarship. W.M. thanks Carlos Peralta for his valuable comments.

#### REFERENCES

- Anderson, J. M. and Streitlien, k. and Barrett, D. S. and Triantafyllou, M. S. "Oscillating foils of high propulsive efficiency". *J. Fluid Mech.*, Vol. 360, 41–72, 1998.
- Blevins, R. D. "Flow-induced vibration". New York, Van Nostrand Reinhold Co., 1977.
- Carmo, B. S. and Sherwin, S. J. and Bearman, P. W. and Willden, R. H. J. "Wake transition in the flow around two circular cylinders in staggered arrangements". *J. Fluid Mech.*, Vol. 597(1), 1–29, 2008.
- Cheng, M. and Chew, Y. T. and Luo, S. C. "Numerical investigation of a rotationally oscillating cylinder in mean flow". *J. Fluid Struct.*, Vol. 15(7), 981–1007, 2001.
- Ellenrieder, K. D. and Parker, K. R. and Soria, J. "Flow structures behind a heaving and pitching finite-span wing". *J. Fluid Mech.*, Vol. 490, 129–138, 2003.
- Freytmuth, P. "Propulsive vortical signature of plunging and pitching airfoils". *AIAA J.*, Vol. 26, 881–883, 1988.
- Gopalan, H. "Numerical Modeling of Aerodynamics of Airfoils of Micro Air Vehicles in Gusty Environment". PhD thesis, University of Akron, 2008.
- Green, S. I. *Fluid Vortices*. Kluwer Academic Publishers, 1995.
- Karniadakis, G. E. and Orszag, S. A. and Israeli, M. "High-order splitting methods for the incompressible Navier-Stokes equations". *J. Comp. Phys.*, Vol. 97, 414–443, 1991.
- Karniadakis, G. E. and Sherwin, S. "Spectral/hp Element Methods for Computational Fluid Dynamics". Oxford University Press, 2005.
- Karniadakis, G. E. and Triantafyllou, G. S. "Frequency Selection and Asymptotic States in Laminar wakes." *J. Fluid Mech.*, Vol. 199(1), 441–469, 1989.
- Lai, J. C. S. and Platzer, M.F. "Jet Characteristics of a Plunging Airfoil". *AIAA J.*, Vol. 37(12), 1529–1537, 1999.
- Li, L. and Sherwin, S. J. and Bearman, P. W. "A moving frame of reference algorithm for fluid/structure interaction of rotating and translating bodies". *Int. J. Numer. Meth. FL.*, Vol. 38, 187–206, 2002.
- Lian, Y. and Shyy, W. "Aerodynamics of Low Reynolds Number Plunging Airfoil Under Gusty Environment". In 45th AIAA Aerospace Sciences Meeting and Exhibit. 8-11 January 2007, Reno, Nevada, Vol. AIAA-2007-71, 2007.
- Medjroubi, W. "Numerical Simulation of the Dynamic Stall for Heaving Airfoils Using Adaptive Mesh Techniques". PhD thesis, University of Oldenburg, Department of Physics, Oldenburg, Germany, 2011a.
- Medjroubi, W. and Stoevesandt, B. and Carmo, B. and Peinke, J. "High-order numerical simulations of the flow around a heaving airfoil". *Computers and Fluids*, Vol. 51(1), 68–84, 2011b.
- Medjroubi, W. and Stoevesandt, B. and Peinke, J. "Wake classification of heaving airfoils using the spectral/hp element method". *Journal of Computational and Applied Mathematics*, Vol. 236(15), 3774–3782, 2012.
- Mittal, R. and Najjar, F. M. "Vortex Dynamics in the Sphere Wake". In 29th AIAA Fluid Dynamics Conference and Exhibit, Norfolk, Virginia, volume 99-3806, 1999.
- Nastase, C. R. and Mavriplis, D. J. "High-order discontinuous Galerkin methods using an hp-multigrid approach". *J. Comp. Phys.*, Vol. 213(1), 330–357, 2006.
- Naudascher, E. and Rockwell, D. "Flow-Induced Vibrations: An Engineering Guide". Rotterdam, Netherlands: Balkema, 1994.
- Ongoren, A. and Rockwell, D. "Flow structure from an oscillating cylinder Part 1. Mechanisms of phase shift and recovery in the near wake". *J. Fluid Mech.*, Vol. 191(1), 197–223, 1988a.
- Ongoren, A. and Rockwell, D. "Flow structure from an oscillating cylinder Part 2. Mode competition in the near wake". *J. Fluid Mech.*, Vol. 191(1), 225–245, 1988b.
- Platzer, M. F. and Jones, K. D. and Young, J. and Lai, J. C. S. "Flapping-Wing Aero dynamics: Progress and Challenges". *AIAA Journal*, Vol. 46(9), 2136–2149, 2008.
- Scanlan, R. H. and Tomko, J. J. "Airfoil and Bridge Deck Flutter Derivatives". *Journal of the Engineering Mechanics Division ASCE*, 97-1717, 1971.
- Schnipper, T. and Andersen, A. and Bohr, T. "Vortex Wakes of a Flapping Foil". *J. Fluid Mech.*, Vol. 633, 411–423,

- 2009.
- Shatalov, A. V. "Numerical Simulation of Incompressible Laminar Flows Using Viscous- Inviscid Interaction Procedure". PhD thesis, University of California, Division Mechanical and Aeronautical Engineering, 2006.
- Williamson, C. H. K. and Govardhan, R. "Vortex-Induced Vibrations". *Annu. Rev. Fluid Mech.*, Vol. 36, 413–55, 2004.
- Williamson, C. H. K. "Fluid Vortices : Vortex Dynamics in the Wake of a Cylinder". *Fluid Vortices*. Kluwer Academic Publishers, 1995.
- Young, J and Lai, J. C. S. "Oscillation Frequency and Amplitude Effects on the Wake of a Plunging Airfoil". *American Institute of Aeronautics and Astronautics*, Vol. 42(10), 2042–2052, 2004.
- Young, J. and Lai, J. C. S. "Frequency and Amplitude Effects in the Wake of a Plunging Airfoil". In 14<sup>th</sup> Australasian Fluid Mechanics Conferences, Adelaide University, Adelaide, Australia. 10-14 December, 2001.
- Young, J. "Numerical simulation of the unsteady aerodynamics of flapping airfoils". PhD thesis, School of Aerospace, Civil and Mechanical Engineering. The University of New South Wales. Australian Defence Force Academy, May 2005.
- Zheng, Z. C. and Zhang, N. "Frequency effects on lift and drag for flow past an oscillating cylinder". *J. Fluid Struct.*, Vol. 24(3), 382–399, 2008.